

Parallel magnetoconductance of interacting electrons in a two-dimensional disordered systemRichard Berkovits¹ and Jan W. Kantelhardt^{1,2,*}¹*Minerva Center and Department of Physics, Bar-Ilan University, Ramat-Gan 52900, Israel*²*Institut für Theoretische Physik III, Universität Giessen, D-35392 Giessen, Germany*

(Received 11 October 2001; published 11 March 2002)

The transport properties of interacting electrons for which the spin degree of freedom is taken into account are numerically studied for small two-dimensional clusters for which the localization length is larger than the system size. On-site electron-electron interactions tend to delocalize the electrons, while long-range interactions enhance localization. On careful examination of the transport properties, we reach the conclusion that it does not show a two-dimensional metal-insulator transition driven by interactions. A parallel magnetic field leads to enhanced resistivity, which saturates once the electrons become fully spin polarized. The strength of the magnetic field for which the resistivity saturates decreases as the electron density goes down. Thus, the numerical calculations capture some of the features seen in recent experimental measurements of parallel magnetoconductance.

DOI: 10.1103/PhysRevB.65.125308

PACS number(s): 73.20.Fz, 71.30.+h, 64.60.Ak

There has been much recent interest in the influence of electron-electron interaction (EEI) on the localization properties of electrons in two-dimensional disordered systems. Behind this renewed interest in the topic are different experimental observations pertaining to the behavior of the conductance of low-density two-dimensional electrons. The conductance exhibits a crossover from an insulatinglike temperature dependence at low densities to a metallic one at higher densities.^{1,2} A second transition back to an insulating dependence at even higher densities was also observed.³ This transition, which is known as the 2DMIT (two-dimensional “metal-insulator” transition), has drawn a flurry of theoretical activity since it is at odds with the prevailing single-parameter scaling theory of localization.⁴ This scaling theory asserts that for noninteracting electrons all states in 2D are localized by any amount of disorder. Since in low-density systems the ratio between the typical interaction energy and the Fermi energy, r_s , is large (i.e., $r_s > 1$), a natural explanation for the 2DMIT is that it is the result of the EEI not taken into account in the original scaling theory. This has prompted an intensive theoretical effort including analytical⁵ and numerical^{6–13} work that tried to explain the 2DMIT as a result of delocalization by the EEI. On the other hand, one may argue that the observed temperature dependence of the conductance is not a result of a metallic zero-temperature phase but rather a manifestation of essentially “high-temperature” physics. Thus, some other physical mechanism (such as traps,¹⁴ interband spin-dependent scattering,^{15,16} temperature-dependent screening,^{17–19} or percolation²⁰) sets a very low-temperature scale and the observed metallic behavior occurs at higher temperatures. Accordingly there is no 2DMIT and the systems are insulating at zero temperature. This viewpoint may find support in some recent experimental results that show a suppression of the 2DMIT once interband scattering is reduced,^{15,16} and from the observation that the bulk of the metallic behavior occurs at temperatures in which there is no quantum interference contributions to the conductance, while weak localization corrections are observed at very low temperatures.^{21–24}

Since it is extremely difficult to go beyond the perturbative treatment of strong EEI in disordered systems, many

numerical studies have been performed in order to clarify the role played by the EEI on the localization properties of disordered systems. While for spinless electrons the EEI qualitatively changes properties of the system such as many-particle energy-level statistics,^{7,8,11,25} persistent current-flow patterns^{9,26–28} and charge-density response to an external perturbation,¹⁰ it does not lead to delocalization of electrons at the Fermi level, which would manifest itself in enhanced conductivity.^{29–31}

The electron-spin degree of freedom nevertheless plays an important role in the so-called 2DMIT. When the influence of the EEI on the conductance of disordered systems is considered using a combination of perturbative and renormalization group techniques³² it leads to the conclusion that there is a divergence in the Cooperon channel at medium interactions, while the ladder channel monotonously decreases as function of the interaction strength. Thus, for polarized (spinless) electrons EEI should indeed decrease the conductance at zero temperature, while the situation for unpolarized electrons is unclear.

The purpose of this paper is to investigate the influence of the EEI on the transport through a disordered system once the spin degree of freedom is taken into account. In previous studies in which spin was considered the effect of EEI on various properties of mesoscopic systems, such as the persistent current^{33–38} and the addition spectrum and spin polarization of quantum dots in the Coulomb blockade regime^{39–46} was studied. In this paper we shall study the role played by EEI on the tunneling amplitude. The tunneling amplitude represents the probability amplitude for injecting an electron into the system at a point \vec{r} with a given energy ε . For a noninteracting system the tunneling amplitude is given by the amplitude of the single-electron eigenfunction with an eigenvalue ε at \vec{r} , while for an interacting system it is defined further on. By evaluating the statistical properties of the tunneling amplitude of an interacting system one obtains information on the localization of the electrons, akin to the properties revealed by the statistics of the wave functions of noninteracting electrons, which is directly connected to the conductance.³¹

The effect of EEI on the localization of the system is quite subtle. While the long-range part of the interaction always enhances the localization of the electrons, the short-range (Hubbard) part tends to delocalize the electrons. Thus, when both interactions are taken into account there is a competing influence, resulting in some delocalization for weak interactions while the localization is enhanced for stronger interactions. Although there are some superficial similarities to the 2DMIT, there are nevertheless some important differences, which in our opinion rule out delocalization due to the Hubbard interaction as an explanation for the 2DMIT. In order for a substantial delocalization to occur the Hubbard interaction must be significantly stronger than the long-range Coulomb part, i.e., the system is in the high-density regime where good screening occurs. Indeed, for any reasonable estimation of interaction parameters, this delocalization occurs for electron densities corresponding to $r_s < 2$, while the 2DMIT occurs at much lower densities corresponding to $r_s \approx 4-20$.

Another striking feature exhibited by some systems for which a 2DMIT was observed is the strong decrease in the conductance once an in-plane magnetic field is applied.⁴⁷⁻⁵² This decrease coincides with the appearance of magnetization^{53,54} and saturates around the point for which the system becomes fully spin polarized. The saturation field decreases as the density goes down and becomes zero at the “metal-insulator” transition point.^{51,52} Naturally, one would like to relate the decrease in conductance to the appearance of spin polarization. In fact, we find that the tunneling amplitude depends on the ground-state spin state once Hubbard interactions are considered, and since the application of an external in-plane magnetic field changes the ground-state spin⁴⁵ it leads to a dependence of the conductance on the spin polarization. We observe a positive magnetoresistance, which is akin in some aspects to the experimental one, as well as saturation of the resistance at a critical magnetic field corresponding to full polarization. Unlike the enhancement in the conductance due to the Hubbard interaction this behavior is robust to the addition of long-range Coulomb interactions. Moreover, the critical magnetic field is reduced as the interaction strength is enhanced (i.e., corresponding to lower densities). Nevertheless, as we shall discuss later, a direct comparison between the numerical and experimental behavior leaves some open questions.

We consider the following tight-binding Hamiltonian:

$$\begin{aligned} \hat{H} = & \sum_{k,j;\sigma} \epsilon_{k,j} n_{k,j;\sigma} - g \mu_B B \hat{S}_z \\ & - V \sum_{k,j;\sigma} [a_{k,j+1;\sigma}^\dagger a_{k,j;\sigma} + a_{k+1,j;\sigma}^\dagger a_{k,j;\sigma} + \text{H.c.}] \\ & + U_H \sum_{k,j} n_{k,j;+1/2} n_{k,j;-1/2} \\ & + U \sum_{k,j>l,p;\sigma,\sigma'} (n_{k,j;\sigma} - K) \\ & \times (n_{l,p;\sigma'} - K) s / |\vec{r}_{k,j} - \vec{r}_{l,p}|, \end{aligned} \quad (1)$$

where $\vec{r} = (k, j)$ denotes a lattice site, $a_{k,j;\sigma}^\dagger$ is an electron creation operator (with spin $\sigma = -\frac{1}{2}, +\frac{1}{2}$), the number operator

is $n_{k,j;\sigma} = a_{k,j;\sigma}^\dagger a_{k,j;\sigma}$, $\epsilon_{k,j}$ is the site energy, chosen randomly between $-W/2$ and $W/2$ with uniform probability, $V = 1$ is a constant hopping matrix element, $K = \nu$ is a positive background charge equal to the electronic filling and s is the lattice constant. As discussed above, there are two types of electron-electron interaction. The Hubbard interaction U_H due to the repulsion of electrons with opposite spin on the same site has a short range only, while the Coulomb interaction U has a long range. We include an in-plane magnetic field B , that couples only to the total z component of the electron spin \hat{S}_z .

We consider systems composed of $N=4$ electrons residing on 6×6 lattices and systems of $N=6$ electrons on 4×4 lattices, corresponding to fillings of $\nu=1/9$ and $3/8$, respectively. We chose $W=5$ and 8 , respectively, so that the single-particle localization length is comparable to the system sizes. Hard-wall boundary conditions are chosen, since the lowest single-electron state for periodic boundary conditions is actually much more delocalized than neighboring states, resulting in an unusual behavior of the conductance close to the fully polarized state.⁵⁵ It is of course not possible here to directly mimic the experimental procedure in which electron density is varied. Instead, the physical content of this density variation can be captured by controlling the ratio of the Fermi energy to the interaction energy. In the present model, it is achieved simply by changing the interaction strengths U and U_H while keeping other parameters constant. The value of U may be related to the electronic density via $U = V\sqrt{4\pi\nu}r_s$. On the other hand, there is no generally accepted value for the ratio between U_H and U for two-dimensional electron gas (2DEG). In Hubbard’s original work the ratio was estimated as $U_H = (10/3)U$ for weakly overlapping hydrogenlike wave functions,⁵⁶ but there is no estimation of the ratio for relevant Si or GaAs samples. We, therefore, will investigate both physical limits, $U/U_H = 1$ and $U/U_H = 0$, as well as other intermediate values.

We carry out our exact diagonalization in the subspace of the total number of electrons N and the total spin component $S_z = M - N/2$ with M being the number of spin-up electrons. Since there is no mechanism for spin flip in the model, the many-particle wave functions with different values of S_z do not interact, and they can be calculated separately by block diagonalization. Using the Lanczos method we obtain the many-particle eigenvalues ϵ_α^{N,S_z} and eigenfunctions $|\alpha^{N,S_z}\rangle$. Because of spin symmetry, as long as $B=0$, $\epsilon_\alpha^{N,-S_z} = \epsilon_\alpha^{N,S_z}$ and $|\alpha^{N,-S_z}\rangle = |\alpha^{N,S_z}\rangle$.

The zero-temperature local tunneling amplitude $\langle 0^N | a_{\vec{r},\sigma}^\dagger | 0^{N-1} \rangle$ between the ground state of N and $N-1$ electrons can be employed here in order to characterize the transport properties of the many-particle interacting system. It has the advantage that only the ground-state energy and eigenvector for N and $N-1$ electrons need to be calculated. The use of the tunneling amplitude in this context has been motivated and substantiated in our previous work.^{31,57} If one compares the tunneling density of states $\nu(\epsilon)$ in the independent-particle approximation on the one hand and for the many-body interacting system on the other hand, it becomes evident that the tunneling amplitude $\langle 0^N | a_{\vec{r},\sigma}^\dagger | 0^{N-1} \rangle$

replaces the single-electron wave function. The same is true for the transmission $t(\vec{r}, \vec{r}', \varepsilon, \sigma)$ of an electron with energy ε and spin σ between two points \vec{r}, \vec{r}' on the interface of the system with external leads, which is related to the conductance $\sigma(\varepsilon)$ through the Landauer formula⁵⁸ $\sigma(\varepsilon) = (e^2/h) \sum_{\vec{r}, \vec{r}', \sigma} |t(\vec{r}, \vec{r}', \varepsilon, \sigma)|^2$, where the sum \vec{r}, \vec{r}' is over all points on the interface. This behavior suggests that the tunneling amplitude is the appropriate quantity to replace the single-electron wave function in studying transport properties of interacting systems. A similar procedure is employed in Ref. 59 in order to generalize the concept of inverse participation ratio for interacting systems.

Note, however, that once interactions are present a many-particle state is a superposition of many different Slater determinants. Hence, the tunneling amplitude is not normalized, as is the single-electron wave function, which is the result of the fact that the spectral weight for interacting systems is not necessarily equal to one. Therefore, in order to study the influence of EEI on quantum localization it is useful to define an effective tunneling amplitude $\phi(\vec{r}, \sigma) = \langle 0^N | a_{\vec{r}, \sigma}^\dagger | 0^{N-1} \rangle / (\sum_{\vec{r}, \sigma} \langle 0^N | a_{\vec{r}, \sigma}^\dagger | 0^{N-1} \rangle^2)^{1/2}$. In the following, the effective tunneling amplitude $\phi(\vec{r}, \sigma)$ is traced for several Hubbard and Coulomb-interaction strengths U_H and U as well as for different in-plane magnetic fields B . In order to analyze the tunneling amplitude and to derive the degree of localization, we calculate the inverse participation ratio $P = \sum_{\vec{r}, \sigma} |\phi(\vec{r})|^4$ averaged over 100 realizations.

It is also possible to discuss the tunneling amplitudes between the lowest eigenvectors of a given spin sector S_z . Of course, when adding an additional electron, the total spin component S_z can either increase or decrease by one half. Denoting the lowest eigenvalue for a given spin sector S_z with N electrons as $|0^{N, S_z}\rangle$, the tunneling amplitudes between the lowest eigenvectors for a given spin sector is $\langle 0^{N, S_z^{\text{final}}} | a_{\vec{r}, \sigma}^\dagger | 0^{N-1, S_z^{\text{initial}}} \rangle$ with $S_z^{\text{final}} = S_z^{\text{initial}} \pm 1/2$ for all values of S_z^{initial} , i.e., $S_z^{\text{initial}} = \frac{1}{2}, \frac{3}{2}$ for $N=4$ and $S_z^{\text{initial}} = \frac{1}{2}, \frac{3}{2}, \frac{5}{2}$ for $N=6$. The results for the corresponding participation ratios are shown in Figs. 1 as a function of U_H without Coulomb interaction ($U=0$). While the tunneling amplitudes of all possible spin channels have very similar increasing for larger Hubbard interaction, indicating weaker localization. In the case of completely polarized electrons, $S_z = \frac{3}{2} \rightarrow 2$ in Fig. 1(a) and $S_z = \frac{5}{2} \rightarrow 3$ in Fig. 1(b), the Hubbard interaction has no effect, since it couples electrons of opposite spin only. It is interesting to note that there seems to be two distinct magnitudes of enhancement. The inverse participation ratios for transitions in which $S_z^{\text{final}} = S_z^{\text{initial}} - 1/2$ are substantially larger than for transitions where $S_z^{\text{final}} = S_z^{\text{initial}} + 1/2$. This may be the result of the fact that for transitions with $S_z^{\text{final}} = S_z^{\text{initial}} - 1/2$ the additional spin-down electron can join many spin-up ‘‘partners,’’ thus enhancing the effectiveness of the Hubbard interaction. For transitions with $S_z^{\text{final}} = S_z^{\text{initial}} + 1/2$ the influence of the Hubbard interaction is diminished, because the relative number of possible pairs of electrons with opposite spin, that can share sites, is reduced. One may also observe that $\langle P^{-1} \rangle$ for the 4×4 lattice shows some decrease for $U_H \geq 5$ V, while for the 6×6

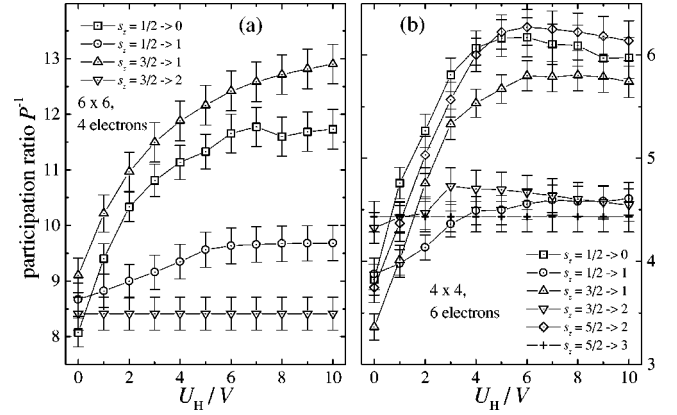


FIG. 1. The participation ratio P^{-1} of the tunneling amplitude for the different spin channels is shown as function of the Hubbard interaction strength U_H for (a) 3 to 4 electrons on a 6×6 lattice, and (b) 5 to 6 electrons on a 4×4 lattice, both without Coulomb interaction. The symbols correspond to the spin transitions: $S_z = \frac{1}{2} \rightarrow 0$ (squares), $\frac{1}{2} \rightarrow 1$ (circles), $\frac{3}{2} \rightarrow 1$ (triangles up), $\frac{3}{2} \rightarrow 2$ (triangles down), $\frac{5}{2} \rightarrow 2$ (diamonds), $\frac{5}{2} \rightarrow 3$ (plus). We have averaged 100 realizations of disorder, and the error bars show the standard deviations of the averages.

lattice $\langle P^{-1} \rangle$ more or less saturates. We attribute this behavior to the fact that for the smaller lattice the electronic density is higher ($\nu=3/8$) resulting in an observable effect of the Mott-Hubbard transition, while for the lower density ($\nu=1/9$) pertaining to the larger lattice the Mott-Hubbard transition is less pronounced.

In order to find out which of the different possible spin channels is relevant for the zero-temperature transport, the energies $\varepsilon_\alpha^{N-1, S_z^{\text{initial}}}$ and $\varepsilon_\alpha^{N, S_z^{\text{final}}}$ of the corresponding multi-particle eigenstates have to be investigated. S_z^{initial} and S_z^{final} have to be selected such, that both energies have their minimal value for each configuration. With no magnetic field, for a ground-state spin value S , all energies $\varepsilon_0^{N-1, S_z} = -S, -S+1, \dots, S-1, S$ are degenerate. Once an infinitesimal magnetic field $B \rightarrow 0^+$ is present (which we assume here), the ground state corresponds to the maximal value of $S_z = S$. Only if the condition $S_z^{\text{final}} = S_z^{\text{initial}} \pm 1/2$ can be fulfilled after this minimizing procedure, the corresponding configuration has nonzero tunneling amplitude at zero temperature.

Figures 2 show the average values of the initial and final spins (open symbols, right scale) for zero-temperature transport as well as the average values of the participation ratio of the corresponding tunneling amplitudes (filled symbols, left scale) as function of the Hubbard interaction U_H , assuming $B \rightarrow 0^+$. For the participation ratios, three different averaging procedures are compared: arithmetic average $\langle P^{-1} \rangle$, typical average $\exp(-\langle \ln P \rangle)$, and geometrical average $1/\langle P \rangle$. They give slightly different values, since the participation ratios are strongly fluctuating. But all of them for both considered systems show the same qualitative behavior: Upon increasing Hubbard interaction, the participation ratios for the zero-temperature transport are increasing as long as $U_H \leq 5$ V, and they become weakly dependent on U_H for larger inter-

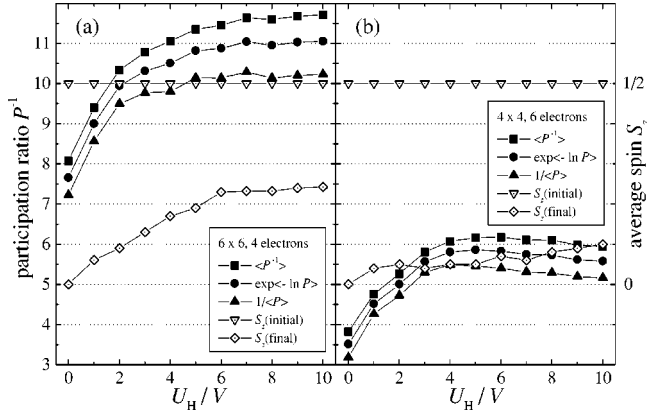


FIG. 2. The average participation ratio P^{-1} of the zero-temperature tunneling amplitude (filled symbols, left axes) and the average initial and final spin S_z (open symbols, right axes) are shown as function of the Hubbard interaction strength U_H for (a) 3 to 4 electrons on a 6×6 lattice, and (b) 5 to 6 electrons on a 4×4 lattice, both without Coulomb interaction. In the averaging procedure, the ground states for both, initial and final state have been chosen as described in the text. For all 100 disorder configurations, the tunneling amplitude is nonzero. For the participation ratios, arithmetical, typical, and geometrical averages are compared.

actions. Hence, the zero-temperature transport in the 2DEG is enhanced by the Hubbard interaction. The enhancement is rather weak, though, reaching about 50% for the 6×6 lattice and 70% for the 4×4 lattice. The range of U_H where the enhancement occurs, cannot be directly compared to the experiments, since the relevant parameter r_s is rather related to the Coulomb interaction U (which is zero here) than to the Hubbard interaction U_H .

Next, we want to investigate, how the zero-temperature transport is affected by an in-plane magnetic field. While there would be some modification of the orbits of electrons for perpendicular magnetic fields (see e.g., Ref. 57) the parallel magnetic field interacts only with the spins of electrons. Since the multiparticle eigenfunctions $|\alpha^{N, S_z}\rangle$ have already been calculated as eigenfunctions of the spin operator \hat{S}_z , their energy levels $\varepsilon_{\alpha}^{N, S_z}$ are just shifted to $\varepsilon_{\alpha}^{N, S_z} - g\mu_B B S_z$ according to Eq. (1). The eigenfunctions $|\alpha^{N, S_z}\rangle$ and the corresponding tunneling amplitudes are not changed, but with $B \neq 0$ a different eigenstate might become the ground state. With increasing B , a higher degree of polarization corresponding to larger S_z becomes favorable.⁴⁵ Figures 3(a) and 3(b) show the average values of the ground-state spins S_z^{initial} (for the three-electron system) and S_z^{final} (for the four-electron system) as function of the in-plane magnetic field B for four values of U_H . In both figures, a monotonously increasing polarization is observed, as expected.

Now, zero-temperature transport can be traced as function of B . One just has to average the participation ratios of the tunneling amplitudes for the corresponding ground states, provided the condition $S_z^{\text{final}} = S_z^{\text{initial}} \pm 1/2$ is fulfilled. If this condition fails, the tunneling amplitude is zero for the corresponding configuration and B . The results of this B -dependent averaging procedure are shown in Fig. 3(c) for

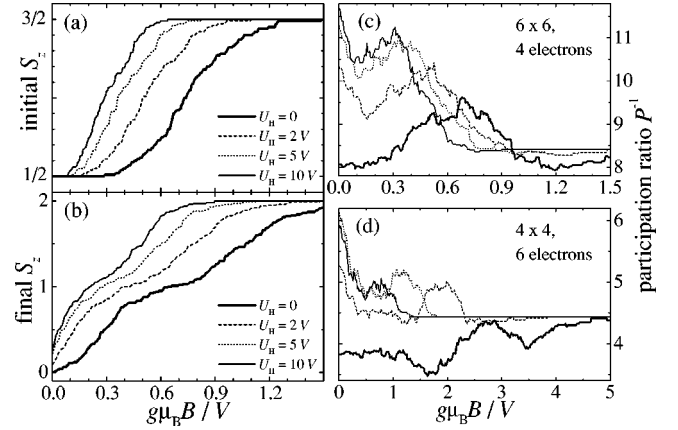


FIG. 3. The average (a) initial and (b) final spins S_z of the ground states are shown vs the scaled magnetic field for 3 to 4 electrons on a 6×6 lattice. With increasing magnetic field, the ground states are moved to higher degrees of polarization. The different lines correspond to different strengths of Hubbard interaction U_H (see legends), while there is no Coulomb interaction. On the right, the average participation ratios $\langle P^{-1} \rangle$ of the zero temperature tunneling amplitude are shown for 3 to 4 electrons on a 6×6 lattice (c) and 5 to 6 electrons on a 4×4 lattice (d). In the (arithmetic) averaging procedure, the ground states for both, initial and final state have been chosen as described in the text. Configurations with zero tunneling amplitude (due to nonmatching spins in initial and final ground states) have been disregarded in the averaging procedures.

3 to 4 electrons on a 6×6 lattice and in Fig. 3(d) 5 to 6 electrons on a 4×4 lattice, again for four values of U_H . In the noninteracting case there is a weak dependence of the conductance on the magnetic field as a result of the weak dependence of $\langle P^{-1} \rangle$ on the single-particle state seen in Figs. 1 for $U_H = 0$. For nonzero Hubbard interaction U_H we observe a drop in $\langle P^{-1} \rangle$ in the range of $g\mu_B B < \Delta$, where Δ is the mean single-particle level spacing. This behavior is the result of the larger participation ratio exhibited by the $S_z^{\text{final}} = S_z^{\text{initial}} - 1/2$ transition compared to the $S_z^{\text{final}} = S_z^{\text{initial}} + 1/2$ transition. As can be seen in Figs. 3, when $g\mu_B B < \Delta/2$, for all realizations, the ground state corresponds to $S_z^{\text{initial}} = 1/2$ for the odd number of electrons, while more and more realizations change from $S_z^{\text{final}} = 0$ to $S_z^{\text{final}} = 1$ as B increases. This leads to the decrease of the participation ratio of the average tunneling amplitude, corresponding to a decrease in the conductance. The initial decrease is followed by intermediate maxima and minima, since, as B increases, the average S_z increases leading to local peaks in the conductance each time that the $S_z^{\text{final}} = S_z^{\text{initial}} - 1/2$ becomes more prevalent. Once a larger portion of realizations become fully polarized (for large magnetic fields B), the conductance drops to the same saturated value for all U_H values. The values B_{sat} of the magnetic field for which the systems become fully polarized are shown in Fig. 4(a) for both system sizes. It can be seen, that B_{sat} decreases with increasing Hubbard interaction U_H , but it never vanishes.

Our findings somewhat resemble the observations of recent experiments:¹ The conductivity of 2DEG semiconductor

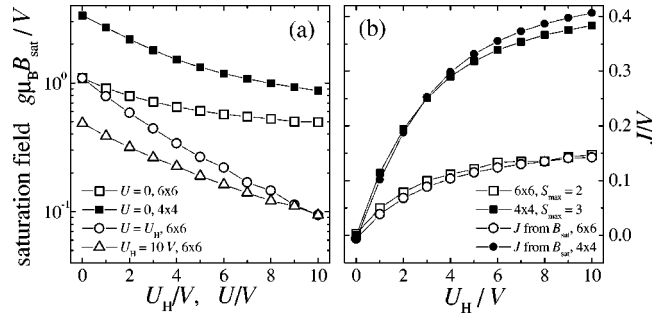


FIG. 4. (a) The saturation field B_{sat} , for which the systems become fully polarized and the average participation ratios P^{-1} of the zero-temperature tunneling amplitude reach their asymptotic value, are shown versus the Hubbard and the Coulomb-interaction strength (see legend). The values of B_{sat} have been averaged for 100 configurations. (b) The values of the average exchange energy J are shown vs U_H for 6×6 systems (open symbols) as well as the 4×4 systems (filled symbols). Two ways to calculate J are compared: (i) J determined from the eigenvalues via Eq. (2) for $B=0$ (squares) and (ii) J obtained from B_{sat} via the discrete version of Eq. (3) (circles). The plot indicates good agreement, justifying the approach to relate B_{sat} to U_H .

devices, that seem to show a “metallic phase,” is reduced with increasing in-plane magnetic field, until a constant conductivity is reached for $B > B_{\text{sat}}$. Although this qualitative behavior is strikingly similar to the results of our calculation, the magnitude of the decrease we observe is much smaller than that in the experiments. For silicon devices decreases by up to two orders of magnitude have been observed depending on the temperature,^{47,48} while for GaAs devices, decreases by a factor of 3 have been reported.^{49,50} Another problem in relating our results to the experiments is the dependence of the saturation field B_{sat} on U_H . In the experiments $B_{\text{sat}} \propto (\nu - \nu_c)^\delta$, where ν_c is the density of the 2DMIT and $\delta=1$ for a wide range of densities,⁵¹ while $\delta \approx 0.6$ close to ν_c elsewhere.⁵² Since we do not identify a metal-insulator transition in our model it is not clear how to directly relate the above experimental observations to our data. Moreover, the experimentally relevant parameter is rather related to the Coulomb interaction U (via r_s) (which is zero here) than to the Hubbard interaction U_H .

Nevertheless, it is possible to relate B_{sat} to U_H using the following consideration: The lowest average energy of the Hamiltonian given in Eq. (1) at a given spin S may be approximated by⁴⁵

$$E(S) - E(0) = \Delta S^2 - JS(S+1) - g\mu_B BS, \quad (2)$$

where J is the averaged exchange energy that depends on U and U_H . Figure 4(b) shows the values of J determined from the eigenvalues $E(S_{\text{max}})$ and $E(0)$ of the systems via Eq. (2) for $B=0$ and $U=0$. A power-law relation $J \propto U_H^\alpha$ with an exponent α in the range from 0.25 to 0.5 may be deduced from our data, and this relation is consistent with results obtained in a previous study of the disordered Hubbard model.⁶⁰ The saturation field B_{sat} corresponds to the field in

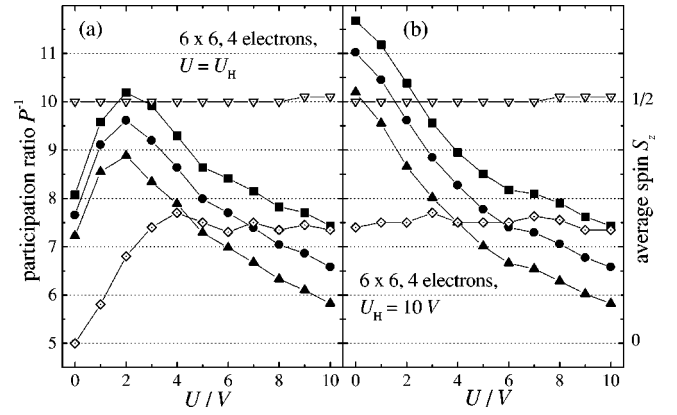


FIG. 5. The average participation ratio P^{-1} of the zero-temperature tunneling amplitude (filled symbols, left axes) and the average initial and final spin S_z (open symbols, right axes) are shown as function of Coulomb interaction strength U , (a) for identical Hubbard interaction $U_H=U$ and (b) for fixed Hubbard interaction $U_H=10 \text{ V}$ for 3 to 4 electrons on a 6×6 lattice. The averaging procedure is the same as for Fig. 2.

which the energy becomes minimal for complete polarization, i.e., $\partial E(S)/\partial S=0$ with $S=S_{\text{max}}$, resulting in

$$g\mu_B B_{\text{sat}} = 2\Delta S_{\text{max}} - J(2S_{\text{max}} + 1). \quad (3)$$

For small values of S it is better to replace the derivative leading to Eq. (3) by the discrete difference leading to $g\mu_B B_{\text{sat}} = \Delta(2S_{\text{max}} - 1) - 2JS_{\text{max}}$. In Fig. 4(b) the value of the averaged exchange energy J obtained from B_{sat} via this equation is compared to the J obtained from the eigenvalues. The figure shows that the relations work reasonably well in describing B_{sat} . Since J increases as function of U_H the saturation field decreases. Thus, the same physics of complete spin polarization at the saturation field describes both the experiment^{51,61} and the numerical results. It is important to note though, that since the exchange⁴⁵ saturates at values lower than Δ , $J(U_H \rightarrow \infty) \approx 0.6\Delta$, there will be no ferromagnetic transition for any value of U_H . This is clear from Fig. 2 where the average value of the spin saturates at low values. Therefore $B_{\text{sat}} \neq 0$ for any value of U_H , and a model with no long-range interactions cannot describe the experimentally observed $B_{\text{sat}} \propto (\nu - \nu_c)^\delta$.

Thus, it is clear that one must move beyond the short-range Hubbard interaction and include a long-range Coulomb interaction in order to present a realistic picture of the 2DMIT behavior. As discussed above there is no established relation between U and U_H , so we shall begin by presenting the highest possible ratio between them, i.e., $U=U_H$. The participation ratio as function of U is presented in Fig. 5(a). An initial enhancement of P^{-1} , which peaks at $U=2 \text{ V}$ is seen, while for larger values of interaction a steady decrease is observed. This behavior is attributed to the interplay between the short- and long-range components of the EEI. Short-range interactions enhance the participation ratio of the tunneling amplitudes, while the long-range interactions suppress it. This is demonstrated in Fig. 5(b) where we keep $U_H=10 \text{ V}$ fixed and tune the value of U . A monotonous

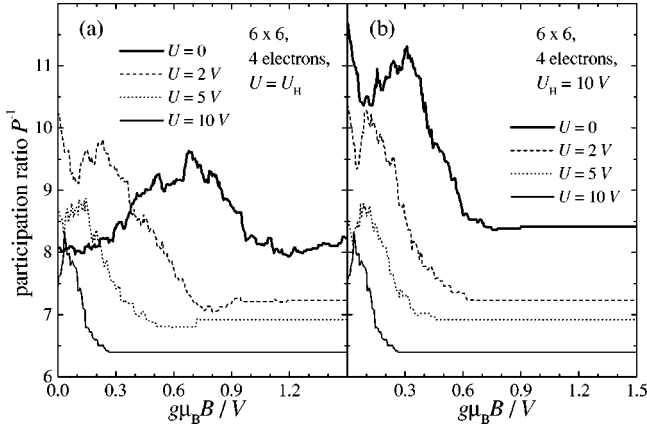


FIG. 6. The average participation ratio $\langle P^{-1} \rangle$ of the zero-temperature tunneling amplitude is shown vs the magnetic field B , (a) for identical Hubbard interaction $U_H = U$ and (b) for fixed Hubbard interaction $U_H = 10$ for 3 to 4 electrons on a 6×6 lattice. The averaging procedure is the same as for Fig. 3.

decrease in P^{-1} as function of U is evident. The influence of the long-range interaction on the spin polarization can also be gleaned from Fig. 5. The short-range interactions lead to spin polarization, while the long-range interaction tends only to slightly nudge the ground-state spin.

The dependence of the participation ratio on the in-plane magnetic field in the presence of long range EEI is depicted in Fig. 6. The main feature of Figs. 3, i.e., the suppression of P^{-1} by the magnetic field and saturation at high magnetic fields remains intact. Thus, long-range Coulomb interactions do not overturn the main conclusions garnered from the magnetoconductance for short-range interactions. The dependence of the saturation field B_{sat} on the Coulomb-interaction strength U shown in Fig. 4(a) is also similar to the dependence on U_H for $U = 0$. There are some differences though. The saturated value of P^{-1} decreases as U becomes stronger, which fits our previous observation that long-range interaction localizes the system. The saturation field depends on the interaction strength, but in contrast to the Hubbard interaction we cannot rule out that $B_{\text{sat}} = 0$ for a finite value of U . If $B_{\text{sat}} = 0$ indeed occurred, the value of interaction for which the field is equal to zero would be much larger than the values of interaction considered here. Since we observe no vanishing of the saturation field, we cannot compare the behavior of B_{sat} to the one seen in the experiment based on the available data.

Once long-range interactions are taken into account one can use the relation $U = V \sqrt{4\pi\nu r_s}$, resulting in a connection between interaction strength and electronic density ν . Since $\nu = 1/9$, the range of interaction strength $U = 0 - 10$ V presented in Figs. 5 corresponds to $r_s \approx 0 - 8.5$. It would be tempting to interpret Fig. 5(a) as a signature of a 2DMIT, but this explanation raises difficulties that make it rather doubtful. The first “transition” from a more insulating behavior to a more metallic one [see Fig. 5(a)] is influenced almost entirely by the Hubbard term as can be seen from its similarity to Figs. 2. At $U \approx 2$ V, the point where the

enhancement due to the short-range interaction saturates, the suppression due to long-range interactions kicks in. This suppression is monotonic and persists at higher values of r_s . The saturation point is determined by U_H , while r_s depends on U . Hence, the corresponding electronic density, for which the peak appears, depends on the ratio of U_H/U . For the lowest possible ratio (i.e., $U_H/U = 1$) the peak occurs at densities corresponding to $r_s \approx 1.7$, which is low compared to the experimentally observed region of metallic behavior¹ corresponding to $r_s \approx 4 - 20$. A higher ratio of U_H/U will result in this peak appearing for even lower values of r_s . Comparing Figs. 5(a) and 5(b) it can be seen that P^{-1} stays approximately constant, when U_H is increased from 2 V to 10 V while $U = 2$ V is kept constant. Only for smaller U , e.g., $U = 1$ V corresponding to $r_s \approx 0.85$, increasing U_H can enhance the tunneling amplitude. Similar behavior has been seen by Selva and Pichard³⁸ for the site occupation number, which gives some indication on the degree of localization in the system. The high densities (low values of r_s) for which the peak in the participation ratio appears, in conjunction with the fact that long-range Coulomb interactions always suppress P^{-1} [see Fig. 5(b)] for any value of r_s lead us to the conclusion that numerical studies of small clusters do not support the notion of an EEI driven metal insulator transition.

On the other hand, the numerical model does seem to reproduce the positive in-plane magnetoresistance and the saturation of the resistance at a critical magnetic field seen in recent experiments.⁴⁷⁻⁵² The physical origin of the saturation is spin polarization of the electron. Similar explanations were proposed for the experimental origin of the saturation.^{51,61} Further studies of higher values of interactions are needed to determine whether quantitative comparison with the experimentally observed $B_{\text{sat}} \propto (\nu - \nu_c)^\delta$ can be obtained. Furthermore, if such behavior was indeed observed, the origin of ν_c would have to be clarified, since it cannot be the critical density of the 2DMIT that is not seen in our model.

Beyond relating our results to existing experimental data, one would like to glean some relevance for possible future experiments. As we pointed out in the introduction the physical situation corresponding to a short range EEI is deep in the metallic regime in which the long-range interaction is perfectly screened. Thus, the enhancement of the conductance in Figs. 2 is not relevant to the existing body of experimental data on the 2DMIT, but it might be relevant to an experimental double gate setup in which the long-range part of the EEI is screened.⁶² According to Figs. 2 the conductance of such a setup should be higher than for a single or no gate set-up for the same 2DEG sample.

In conclusion, the conductance of interacting electrons for which the spin degree of freedom is taken into account exhibits an intricate dependence upon EEI and parallel magnetic field. Hubbard on-site interactions enhance the conductance while long-range Coulomb interactions suppress it. The interplay between the two can lead to a region of enhanced conductance, but this region is at densities corresponding to $r_s \approx 1$, which are too high to be relevant to the 2DMIT. For lower densities corresponding to higher values of r_s the con-

ductance is suppressed. A parallel magnetic field reduces the conductance until it saturates once the electrons become fully spin polarized. The saturation field decreases for lower electron density. These features are seen in recent experimental measurements of parallel magnetoconductance. Further investigation, at higher values of interaction, are needed in

order to clarify whether other features may be explained by this model.

R.B. thanks the Israel Science Foundations Centers of Excellence Program and J.K. thanks the Minerva Foundation and the Deutsche Akademische Austauschdienst (DAAD) for financial support.

*Present address: Center for Polymer Studies and Department of Physics, Boston University, Boston, MA 02215.

¹For a recent review see, E. Abrahams, S.V. Kravchenko, and M.P. Sarachik, *Rev. Mod. Phys.* **73**, 251 (2001).

²S.V. Kravchenko, G.V. Kravchenko, J.E. Furneaux, V.M. Pudalov, and M. D'Iorio, *Phys. Rev. B* **50**, 8039 (1994); S.V. Kravchenko, W.E. Mason, G.E. Bowker, J.E. Furneaux, V.M. Pudalov, and M. D'Iorio, *ibid.* **51**, 7038 (1995); P.T. Coleridge, R.L. Williams, Y. Feng, and P. Zawadzki, *ibid.* **56**, R12 764 (1997); D. Popovic, A.B. Fowler, and S. Washburn, *Phys. Rev. Lett.* **79**, 1543 (1997); V.M. Pudalov, *JETP Lett.* **66**, 175 (1997); Y. Hanein, U. Meirav, D. Shahar, C.C. Li, D.C. Tsui, and H. Shtrikman, *Phys. Rev. Lett.* **80**, 1288 (1998); J. Yoon, C.C. Li, D. Shahar, D.C. Tsui, and M. Shayegan, *ibid.* **82**, 1744 (1999).

³A.R. Hamilton, M.Y. Simmons, M. Pepper, E.H. Linfield, P.D. Rose, and D.A. Ritchie, *Phys. Rev. Lett.* **82**, 1542 (1999).

⁴E. Abrahams, P.W. Anderson, D.C. Licciardello, and T.V. Ramakrishnan, *Phys. Rev. Lett.* **42**, 673 (1979).

⁵V. Dobrosavljevic, E. Abrahams, E. Miranda, and S. Chakravarty, *Phys. Rev. Lett.* **79**, 455 (1997); C. Castellani, C. DiCastro, and P.A. Lee, *Phys. Rev. B* **57**, 9381 (1998); Q. Si and C.M. Varma, *Phys. Rev. Lett.* **81**, 4951 (1998); S. Chakravarty, L. Yin, and E. Abrahams, *Phys. Rev. B* **58**, 559 (1998); T.R. Kirkpatrick and D. Belitz, *ibid.* **62**, 966 (2000).

⁶F.G. Pikus and A.L. Efros, *Solid State Commun.* **92**, 485 (1994).

⁷J. Talamanes, M. Pollak, and L. Elam, *Europhys. Lett.* **35**, 511 (1996).

⁸E. Cuevas, *Phys. Rev. Lett.* **83**, 140 (1999).

⁹G. Benenti, X. Waintal, and J.-L. Pichard, *Phys. Rev. Lett.* **83**, 1826 (1999).

¹⁰X. Waintal, G. Benenti, and J.-L. Pichard, *Europhys. Lett.* **49**, 466 (2000).

¹¹D.L. Shepelyansky, *Phys. Rev. B* **61**, 4588 (2000); D.L. Shepelyansky and P.H. Song, *Ann. Phys. (Leipzig)* **8**, 665 (1999).

¹²P.J.H. Denteneer, R.T. Scalettar, and N. Trivedi, *Phys. Rev. Lett.* **83**, 4610 (1999).

¹³T. Vojta, F. Epperlein, S. Kilina, and M. Schreiber, *Phys. Status Solidi B* **218**, 31 (2000).

¹⁴B.L. Altshuler and D.L. Maslov, *Phys. Rev. Lett.* **82**, 185 (1999).

¹⁵S.J. Papadakis, E.P. De Poortere, H.C. Manoharan, M. Shayegan, and R. Winkler, *Science* **283**, 2056 (1999).

¹⁶Y. Yaish, O. Prus, E. Buchstab, S. Shapira, G. Ben Yoseph, U. Sivan, and A. Stern, *Phys. Rev. Lett.* **84**, 4954 (2000).

¹⁷T.M. Klapwijk and S. Das Sarma, *Solid State Commun.* **110**, 581 (1999).

¹⁸S. Das Sarma and H.E. Hwang, *Phys. Rev. Lett.* **83**, 164 (1999).

¹⁹G. Zala, B.N. Narozhny, and I.L. Aleiner, *Phys. Rev. B* **64**, 214204 (2001).

²⁰Y. Meir, *Phys. Rev. Lett.* **83**, 3506 (1999).

²¹M.Y. Simmons, A.R. Hamilton, M. Pepper, E.H. Linfield, P.D.

Rose, and D.A. Ritchie, *Phys. Rev. Lett.* **84**, 2489 (2000).

²²V. Senz, T. Heinzl, T. Ihn, K. Ensslin, G. Dehlinger, D. Gruetzmacher, and U. Gennser, *Phys. Rev. B* **61**, R5082 (2000).

²³B.L. Altshuler, G.W. Martin, D.L. Maslov, V.M. Pudalov, A. Prinz, G. Brunthaler, and G. Bauer, *Phys. Rev. Lett.* **86**, 4895 (2001).

²⁴Y.Y. Proskuryakov, A.K. Savchenko, S.S. Safonov, M. Pepper, M.Y. Simmons, and D.A. Ritchie, *Phys. Rev. Lett.* **86**, 4895 (2001).

²⁵R. Berkovits, *Europhys. Lett.* **25**, 681 (1994).

²⁶R. Berkovits and Y. Avishai, *Phys. Rev. B* **57**, R15 076 (1998).

²⁷F. Selva and D. Weinmann, *Eur. J. Biochem.* **18**, 137 (2000).

²⁸G. Benenti, X. Waintal, and J.-L. Pichard, *Europhys. Lett.* **51**, 89 (2000).

²⁹R. Berkovits and Y. Avishai, *Phys. Rev. Lett.* **76**, 291 (1996).

³⁰T. Vojta, F. Epperlein, and M. Schreiber, *Phys. Rev. Lett.* **81**, 4212 (1998).

³¹R. Berkovits, J.W. Kantelhardt, Y. Avishai, S. Havlin, and A. Bunde, *Phys. Rev. B* **63**, 085102 (2001).

³²A.M. Finkelstein, *Z. Phys. B: Condens. Matter* **56**, 189 (1984); C. Castellani, C. DiCastro, P.A. Lee, and M. Ma, *Phys. Rev. B* **30**, 527 (1984).

³³M. Ramin, B. Reulet, and H. Bouchiat, *Phys. Rev. B* **51**, 5582 (1995).

³⁴M. Kamal, Z.H. Musslimani, and A. Auerbach, *J. Phys. I* **5**, 1481 (1995).

³⁵R.A. Römer and A. Punnoose, *Phys. Rev. B* **52**, 14 809 (1995).

³⁶Q.H. Wang, Z.D. Wang, and J.X. Zhu, *Phys. Rev. B* **54**, 8101 (1996).

³⁷R. Kotlyar and S. Das Sarma, *Phys. Rev. Lett.* **86**, 2388 (2001).

³⁸F. Selva and J.-L. Pichard, *Europhys. Lett.* **55**, 518 (2001).

³⁹O. Prus, A. Auerbach, Y. Aloni, U. Sivan, and R. Berkovits, *Phys. Rev. B* **54**, 14 289 (1996).

⁴⁰R. Berkovits, *Phys. Rev. Lett.* **81**, 2128 (1998).

⁴¹P.W. Brouwer, Y. Oreg, and B.I. Halperin, *Phys. Rev. B* **60**, R13 977 (1999).

⁴²E. Eisenberg and R. Berkovits, *Phys. Rev. B* **60**, 15 261 (1999).

⁴³H.U. Baranger, D. Ullmo, and L.I. Glazman, *Phys. Rev. B* **61**, R2425 (2000).

⁴⁴P. Jacquod and A.D. Stone, *Phys. Rev. Lett.* **84**, 3938 (2000).

⁴⁵I.L. Kurland, R. Berkovits, and B.L. Altshuler, *Phys. Rev. Lett.* **86**, 3380 (2001).

⁴⁶G. Benenti, G. Caldera, and D.L. Shepelyansky, *Phys. Rev. Lett.* **86**, 5333 (2001).

⁴⁷D. Simonian, S.V. Kravchenko, M.P. Sarachik, and V.M. Pudalov, *Phys. Rev. Lett.* **79**, 2304 (1997).

⁴⁸V.M. Pudalov, G. Brunthaler, A. Prinz, and G. Bauer, *JETP Lett.* **65**, 932 (1997).

⁴⁹M.Y. Simmons, A.R. Hamilton, M. Pepper, E.H. Linfield, P.D.

- Rose, D.A. Ritchie, A.K. Savchenko, and T.G. Griffiths, *Phys. Rev. Lett.* **80**, 1292 (1998).
- ⁵⁰J. Yoon, C.C. Li, D. Shahar, D.C. Tsui, and M. Shayegan, *Phys. Rev. Lett.* **84**, 4421 (2000).
- ⁵¹A.A. Shashkin, S.V. Kravchenko, V.T. Dolgoplov, and T.M. Klapwijk, *Phys. Rev. Lett.* **87**, 086801 (2001).
- ⁵²S.A. Vitkalov, H. Zheng, K.M. Mertes, M.P. Sarachik, and T.M. Klapwijk, *Phys. Rev. Lett.* **87**, 086401 (2001).
- ⁵³T. Okamoto, K. Hosoya, S. Kawaji, and A. Yagi, *Phys. Rev. Lett.* **82**, 3875 (1999).
- ⁵⁴S. Vitkalov, H. Zheng, K.M. Mertes, M.P. Sarachik, and T.M. Klapwijk, *Phys. Rev. Lett.* **85**, 2164 (2000).
- ⁵⁵R. Berkovits and J.W. Kantelhardt, *Phys. Status Solidi B* (to be published).
- ⁵⁶J. Hubbard, *Proc. R. Soc. London, Ser. A* **276**, 238 (1963).
- ⁵⁷J.W. Kantelhardt, R. Berovits, and Y. Avishai, *Physica A* **302**, 359 (2001).
- ⁵⁸R. Landauer, *IBM J. Res. Dev.* **1**, 233 (1957); M. Büttiker, *Phys. Rev. Lett.* **57**, 1761 (1986).
- ⁵⁹G.S. Jeon, S. Wu, H.-W. Lee, and M.Y. Choi, *Phys. Rev. B* **59**, 3033 (1999).
- ⁶⁰J.A. Folk, C.M. Marcus, R. Berkovits, I.L. Kurland, I.L. Aleiner, and B.L. Altshuler, *Phys. Scr., T* **T90**, 26 (2001).
- ⁶¹V.T. Dolgoplov and A. Gold, *JETP Lett.* **71**, 27 (2001).
- ⁶²We thank Y. Gefen for pointing out the double-gate setup as a practical way to screen the long-range component of the EEI.